CHINESE OPTICS LETTERS

Vol. 21, No. 10 | October 2023

Optimal initial states for quantum parameter estimation based on Jaynes–Cummings model [Invited]

Liwen Qiao (乔莉文)[1], Jia-Xin Peng (彭家鑫)[1,2], Baiqiang Zhu (朱百强)[1,2], Weiping Zhang (张卫平)[2,3,4,5], and Keye Zhang (张可烨)[1,2*]

[1] Quantum Institute for Light and Atoms, State Key Laboratory of Precision Spectroscopy, Department of Physics, School of Physics and Electronic Science, East China Normal University, Shanghai 200062, China

[2] Shanghai Branch, Hefei National Laboratory, Shanghai 201315, China

[3] School of Physics and Astronomy, and Tsung-Dao Lee Institute, Shanghai Jiao Tong University, Shanghai 200240, China

[4] Shanghai Research Center for Quantum Sciences, Shanghai 201315, China

[5] Collaborative Innovation Center of Extreme Optics, Shanxi University, Taiyuan 030006, China

*Corresponding author: kyzhang@phy.ecnu.edu.cn

Received April 18, 2023 | Accepted May 31, 2023 | Posted Online October 7, 2023

Quantum parameter estimation is a crucial tool for inferring unknown parameters in physical models from experimental data. The Jaynes–Cummings model is a widely used model in quantum optics that describes the interaction between an atom and a single-mode quantum optical field. In this Letter, we systematically investigate the problem of estimating the atom-light coupling strength in this model and optimize the initial state in the full Hilbert space. We compare the precision limits achievable for different optical field quantum states, including coherent states, amplitude- and phase-squeezed states, and provide experimental suggestions with an easily prepared substitute for the optimal state. Our results provide valuable insights into optimizing quantum parameter estimation in the Jaynes–Cummings model and can have practical implications for quantum metrology with hybrid quantum systems.

Keywords: quantum Fisher information; Jaynes–Cummings model; parameter estimation theory.
DOI: 10.3788/COL202321.102701

1. Introduction

Quantum metrology is a thriving interdisciplinary field that combines measurement techniques with quantum mechanics to achieve high-precision measurement of various physical observables, such as force, velocity, mass, and temperature[1–3]. However, several physical quantities of interest may be impossible to measure directly, leading to the development of parameter estimation theory[4–7]. Quantum parameter estimation, already a vital subfield of quantum metrology, focuses on indirectly inferring such quantities from data samples. The precision of the resulting estimation can be determined using quantum Fisher information (QFI), as the inverse of QFI sets the lower limit on the estimation error[4–7]. As a result, pursuing the maximum QFI is a fundamental aspect of quantum parameter estimation theory, as it provides the most optimal limit on precision achievable with all available resources[3,8–10].

Over the past few decades, there has been a continuous emergence of fruitful research in the field of quantum parameter estimation, including studies on phase estimation in quantum interferometers[11–13], estimation of magnetic field-related parameters[10,14,15], and estimation of coupling strength in various interaction models[16–18]. In some scenarios, it is necessary to estimate multiple parameters simultaneously, as in quantum imaging, which has driven the development of quantum multiparameter estimation[3,19–24], e.g., simultaneous estimation of the positions of two non-coherent point sources[25–28], simultaneous estimation of rotating magnetic field strength and frequency[14], and multiple phase estimation[29–33]. Even today, quantum parameter estimation remains a vibrant field of research.

The Jaynes–Cummings (J–C) model is a widely used model in the field of quantum optics, and it is used to describe the interaction between a single-mode optical field and a two-level system[34,35]. Despite its simplicity, it has been successfully applied to the study of various quantum effects, such as entanglement[36–38], collapse and revival of a population[39], and quantum teleportation[40–42]. The study of the parametric estimation problem based on the J–C model is not only essential for the development of the applicability of quantum parameter estimation theory but also contributes to an in-depth understanding of the quantum enhancement effect on precise measurements.

© 2023 Chinese Optics Letters

One of the early works in this direction was by Genoni *et al.* in 2012 who studied the estimation of the coupling constant in the J–C model. They found that the QFI is related to the excitation number of the probe and is independent of the parameters to be estimated, and they provided an optimal measurement strategy[43]. More recently, Allati *et al.* extended the parameter estimation problem in the J–C model to estimate the weight and initial phase of the initial state and used Shannon entropy to investigate the relationship between quantum entanglement and QFI[44]. Moreover, there have been efforts to study multiparameter estimation in the J–C model. For instance, recently, Houssaoui *et al.* demonstrated that the average number of photons, the number of photons inside the cavity, the dimensionless detuning parameter, and the dimensionless time parameter can be estimated simultaneously[45]. These studies highlight the importance and versatility of using the J–C model in quantum metrology research.

It is important to note that previous research on parameter estimation in the J–C model has been limited to a single subspace of the complete quantum state space of the composite system, composed of a two-level atom and a single-mode optical field. To fill this research gap, we investigate the estimation of coupling strength from a full Hilbert space perspective. Our study reveals that the optimization problem of coupling strength estimation in the whole space can be simplified into two parts: the optimization of the quantum state in each subspace and the optimization of the probability distribution of individual subspaces in the whole Hilbert space. From this, we obtain the ultimate precision limit for estimating coupling strength under the J–C model. Additionally, we consider the influence of different typical quantum states of the optical field, i.e., photon number statistical distributions, on the estimation precision. Notably, we find that when the optical field resonates with the atom, the coherent state is the optimal initial state for estimating the coupling strength, as it provides the highest estimation precision. This study sheds light on parameter estimation and initial state optimization problems of composite quantum systems involving atom-light interaction.

2. Background

2.1. Quantum Fisher information based on generator

In order to facilitate readers' understanding of the current work, let us first briefly review the relevant theories for calculating the QFI based on the generator method. For a closed system, suppose the system is initially prepared in the state $|\psi_0\rangle$. Evolved for a period of time under the action of Hamiltonian $\hat{H}(g)$, the output state reads as $|\psi_g\rangle = \hat{U}_g|\psi_0\rangle$. Here, $\hat{U}_g = e^{-i\hat{H}(g)t}$ is the parameter-dependent time evolution operator. According to the definition of QFI, one can easily obtain

$$F_g = 4(\langle\partial_g\psi_g|\partial_g\psi_g\rangle - |\langle\psi_g|\partial_g\psi_g\rangle|^2), \tag{1}$$

where F_g denotes the QFI about unknown parameter g. Therefore, the lower bound of the variance when estimating g satisfies[4–7]

$$\langle\Delta^2\hat{g}\rangle \geq 1/\nu F_g. \tag{2}$$

This is the famous Cramér–Rao inequality. Here, ν is the number of resources used in the estimation procedure, e.g., the number of estimate protocol repetitions.

The Hermitian operator[10,46,47] is defined as

$$\hat{h}_g^{\mathrm{H}} = i(\partial_g\hat{U}_g^{\dagger})\hat{U}_g, \tag{3}$$

namely, the form of the generator of the local parameter translation about g, in which the superscript "H" indicates that we are working with the Heisenberg representation. Further, we substitute Eq. (3) into Eq. (1) to obtain[3]

$$F_g = 4[\langle\psi_0|(\hat{h}_g^{\mathrm{H}})^2|\psi_0\rangle - \langle\psi_0|\hat{h}_g^{\mathrm{H}}|\psi_0\rangle^2] = 4\langle\psi_0|(\Delta\hat{h}_g^{\mathrm{H}})^2|\psi_0\rangle. \tag{4}$$

The above formula indicates that, for a closed system, the QFI of the pure state is proportional to the variance of the generator. In particular, when selecting the initial state as $|\psi_0\rangle = \frac{1}{\sqrt{2}}[|\lambda_{\max}(\hat{h}_g^{\mathrm{H}})\rangle + e^{i\phi}|\lambda_{\min}(\hat{h}_g^{\mathrm{H}})\rangle]$[46,48], the maximum quantum QFI is obtained, i.e.,

$$F_{g,\mathrm{Max}} = [\lambda_{\max}(\hat{h}_g^{\mathrm{H}}) - \lambda_{\min}(\hat{h}_g^{\mathrm{H}})]^2, \tag{5}$$

where $\lambda_{\max}(\hat{h}_g^{\mathrm{H}})$ $[\lambda_{\min}(\hat{h}_g^{\mathrm{H}})]$ is the maximum (minimum) eigenvalue of $\hat{h}_g^{\mathrm{H}}$, and $|\lambda_{\max}(\hat{h}_g^{\mathrm{H}})\rangle$ $[|\lambda_{\min}(\hat{h}_g^{\mathrm{H}})\rangle]$ is the corresponding eigenstate. Note that the relative phase ϕ in the initial state has no effect on the first- and second-order moments of the generator, and thus does not affect the maximum QFI. Thus, the highest estimation precision of the unknown parameter g is completely determined by the properties of the generator $\hat{h}_g^{\mathrm{H}}$.

2.2. Jaynes–Cummings model

The J–C model describes the interaction between a single-mode optical field and a two-level atom, which is described by Hamiltonian ($\hbar = 1$)[34,35],

$$\hat{H} = \frac{\omega_0}{2}\hat{\sigma}_z + \omega\hat{a}^{\dagger}\hat{a} + g(\hat{\sigma}_+\hat{a} + \hat{a}^{\dagger}\hat{\sigma}_-), \tag{6}$$

where ω_0 denotes the atomic transition frequency, ω is frequency of the optical mode, g describes the coupling strength between the optical field and the atom, $\hat{\sigma}_{x,y,z}$ are the Pauli matrices, and $\hat{\sigma}_{\pm} = (\hat{\sigma}_x \pm i\hat{\sigma}_y)/2$ denotes the flip-up (flip-down) operator. Once the excitation number operator $\hat{N} = \hat{a}^{\dagger}\hat{a} + \hat{\sigma}_+\hat{\sigma}_-$ is defined, then we can divide the state space of the J–C model into a series of direct sums of subspaces[34,35]. The reason is that the total number of particles (N) corresponding to operator $\hat{N}$ in each subspace is determined. For a subspace with a value of

$N = n$, the basis vectors in the subspace are $|e,n-1\rangle$ and $|g,n\rangle$. Therefore, the Hamiltonian $\hat{H}$ in this subspace is expressed as ($\hat{\sigma}_z$ representation)

$$\hat{H}_N = \begin{bmatrix} (N-\frac{1}{2})\omega + \frac{1}{2}\Delta & g\sqrt{N} \\ g\sqrt{N} & (N-\frac{1}{2})\omega - \frac{1}{2}\Delta \end{bmatrix} = g\sqrt{N}\hat{\sigma}_1 + \frac{1}{2}\Delta\hat{\sigma}_3, \tag{7}$$

where $\Delta = \omega_0 - \omega$ is the detuning of the atom and the optical field, the subscript "N" in $\hat{H}_N$ means that the total excitation number of this subspace is N, and $\hat{\sigma}_{1,2,3}$ are

$$\hat{\sigma}_1 = \begin{bmatrix} 0 & 1 \\ 1 & 0 \end{bmatrix}, \quad \hat{\sigma}_2 = \begin{bmatrix} 0 & -i \\ i & 0 \end{bmatrix}, \quad \hat{\sigma}_3 = \begin{bmatrix} 1 & 0 \\ 0 & -1 \end{bmatrix}. \tag{8}$$

Note the distinction between $\hat{\sigma}_{x,y,z}$, which only describes the atom, and $\hat{\sigma}_{1,2,3}$, which describes a composite system composed of an atom and an optical field. For the convenience of subsequent discussions, we specify the subspace with a total excitation number of N as the Nth subspace.

3. Estimation of Coupling Strength in the Jaynes–Cummings Model

Currently, we take the coupling strength g as the parameter to be estimated. We first discuss the estimation of g in a single subspace of the J–C model, and then turn to the estimation of g in the whole Hilbert space.

3.1. Estimation of coupling strength in subspaces

Based on Eqs. (3) and (7), one can obtain the generator of the Nth subspace,

$$\hat{h}_g^{\mathrm{H},N} = c_1\hat{\sigma}_1 + c_2\hat{\sigma}_2 + c_3\hat{\sigma}_3, \tag{9}$$

with

$$c_1 = -\frac{\sqrt{N}[4Ntg^2\Omega + \Delta^2\sin(t\Omega)]}{\Omega^3}, \quad c_2 = -\frac{\Delta\sqrt{N}[1-\cos(t\Omega)]}{\Omega^2}, \quad c_3 = -\frac{2N\Delta g[t\Omega^2 - \Omega\sin(t\Omega)]}{\Omega^4}. \tag{10}$$

Here, $\Omega = \sqrt{\Delta^2 + 4Ng^2}$ denotes the Rabi frequency.

In theory, the optimal state at this point should be the equal weight superposition of the two eigenstates of $\hat{h}_g^{\mathrm{H},N}$. Unfortunately, the current optimal state contains the parameter g to be estimated, which needs to be adaptively prepared. Moreover, it is very difficult to find the state without the parameter g that maximizes the variance of $\hat{h}_g^{\mathrm{H},N}$ (note that the optimal state is not unique; this is because the phase between the eigenstates of the two generators can be arbitrary). Obviously, this creates limitations for practical applications.

Interestingly, one finds that at the long-term limit, $\hat{h}_g^{\mathrm{H},N}$ can be approximately written as

$$\hat{h}_g^{\mathrm{H},N} \approx d_1\hat{\sigma}_1 + d_3\hat{\sigma}_3 \tag{11}$$

with

$$d_1 = -\frac{4\sqrt{N^3}g^2t}{\Omega^2}, \quad d_3 = -\frac{2N\Delta gt}{\Omega^2}. \tag{12}$$

This is because when the time is very long, the part that is proportional to t in Eq. (10) dominates. After normalizing long-term $\hat{h}^{\mathrm{H},N}$ in Eq. (11), we get

$$\hat{h}_g^{\mathrm{H},N} = -\frac{2Ngt}{\Omega}\vec{n}\cdot\vec{\sigma}, \tag{13}$$

where $\vec{n} = (\frac{2g\sqrt{N}}{\Omega}, 0, \frac{\Delta}{\Omega})$ is the unit vector. In particular, although $\vec{n}$ also contains g, one can easily find a vector orthogonal to $\vec{n}$, such as the eigenstate of $\hat{\sigma}_2$, which ensures the maximum variance of $\hat{h}_g^{\mathrm{H},N}$. Therefore, under the long-term limit, the optimal initial state of the estimated g in the Nth subspace is approximately

$$|\psi_{0,\mathrm{Max}}^{(N)}\rangle = \frac{1}{\sqrt{2}}(|e,N-1\rangle + i|g,N\rangle). \tag{14}$$

According to Eqs. (5) and (11), the maximum QFI for estimating coupling strength in the Nth subspace is given by

$$F_{g,\mathrm{Max}}^{(N)} = \frac{16N^2g^2t^2}{\Omega^2}. \tag{15}$$

Figure 1 depicts the set of optimal initial states for estimating g under the Bloch sphere representation, in which Figs. 1(a) and 1(b) correspond to short and long times, respectively. We can

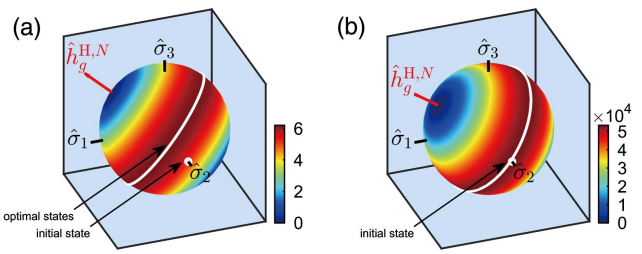

Fig. 1. Red vector represents the direction of the generated $\hat{h}_g^{\mathrm{H},N}$ on the Bloch sphere. The white curve corresponds to the set of quantum states that are orthogonal to $\hat{h}_g^{\mathrm{H},N}$ and maximize its variance. (a) At a small time scale of $gt = 1$, the eigenstates of $\hat{\sigma}_2$ (marked as white dots) do not belong to the optimal state set. (b) At a longer time scale of $gt = 100$, the eigenstate of $\hat{\sigma}_2$ lies on the white curve, indicating that the state is one of the optimal initial states. Here, we take $N = 1$ and $\Delta = 2g$.

clearly see that the eigenstate of $\hat{\sigma}_2$ is indeed the optimal state when the time is long. Therefore, in the following discussion, we discuss the estimation problem under the condition of long-time parameterization.

3.2. Estimation of coupling strength in whole Hilbert space

In the J–C model, the direct-sum space of each subspace constitutes the whole Hilbert space. Hence, the quantum state of the whole space can be written as the direct-sum of all subspace quantum states, i.e.[49,50],

$$|\psi_0\rangle = \bigoplus_{N=0}^{\infty} C_N |\psi_0^{(N)}\rangle, \tag{16}$$

where C_N is the probability amplitude of the excitation number operator in the Nth subspace, satisfying $\sum_{N=0}^{\infty} P_N = 1$ and in which $P_N = |C_N|^2$ denotes the probability distribution of the Nth subspace. Notice that the basis vector of the subspace with $N = 0$ is $|g, 0\rangle$, which does not participate in the evolution of the quantum state and then does not give the quantum state information about g. In addition, the generator $\hat{h}_g^{\mathrm{H},N}$ is naturally 0 when $N = 0$.

Similarly, the total generator can be expressed as[49,50]

$$\hat{h}_g^{\mathrm{H}} = \bigoplus_{N=0}^{\infty} \hat{h}_g^{\mathrm{H},N}. \tag{17}$$

Insert Eqs. (16) and (17) into Eq. (4) and we obtain the expression of the QFI for the total Hilbert space,

$$\mathcal{F}_g = 4\left[\sum_{N=0}^{\infty} P_N \langle\psi_0^{(N)}|(\hat{h}_g^{\mathrm{H},N})^2|\psi_0^{(N)}\rangle\right] - 4\left(\sum_{N=0}^{\infty} P_N \langle\psi_0^{(N)}|\hat{h}_g^{\mathrm{H},N}|\psi_0^{(N)}\rangle\right)^2. \tag{18}$$

Note that owing to the second term on the right side, $\mathcal{F}_g$ is not a simple summation of the QFI for each subspace, which is

$$\mathcal{F}_g^{(N)} = 4[P_N \langle\psi_0^{(N)}|(\hat{h}_g^{\mathrm{H},N})^2|\psi_0^{(N)}\rangle] - 4(P_N \langle\psi_0^{(N)}|\hat{h}_g^{\mathrm{H},N}|\psi_0^{(N)}\rangle)^2. \tag{19}$$

This indicates that there may be associations between different subspaces. In particular, one can see that the $\mathcal{F}_g$ depends on the quantum state of each subspace and the probability distribution P_N. Therefore, the optimization of $\mathcal{F}_g$ can be divided into two steps: the first step is to optimize the quantum state of each subspace, and the other is to optimize the probability distribution P_N.

3.2.1. Optimization of the subspace quantum state

In Eq. (18), we notice that the expected value of the square of $\hat{h}_g^{\mathrm{H},N}$ is independent of the subspace quantum state (see first term), while the square of the sum of $\hat{h}_g^{\mathrm{H},N}$ expected value is always non-negative (see second term). Therefore, the optimization goal of the subspace quantum state is to make the second term of Eq. (18) equal to 0, that is $\sum_{N=0}^{\infty} P_N \langle\psi_0^{(N)}|\hat{h}_g^{\mathrm{H},N}|\psi_0^{(N)}\rangle = 0$. Obviously, when the quantum state of each subspace is in the optimal initial state, i.e., $\langle\psi_{0,\mathrm{Max}}^{(N)}|\hat{h}_g^{\mathrm{H},N}|\psi_{0,\mathrm{Max}}^{(N)}\rangle = 0$, the optimization of the subspace quantum state is completed. Furthermore, the $\mathcal{F}_g$ of the whole space is simplified as

$$\mathcal{F}_g^{\mathrm{O}} = \sum_{N=0}^{\infty} P_N F_{g,\mathrm{Max}}^{(N)}, \tag{20}$$

where $F_{g,\mathrm{Max}}^{(N)} = 4\langle\psi_{0,\mathrm{Max}}^{(N)}|(\hat{h}_g^{\mathrm{H},N})^2|\psi_{0,\mathrm{Max}}^{(N)}\rangle$, owing to $\langle\psi_{0,\mathrm{Max}}^{(N)}|\hat{h}_g^{\mathrm{H},N}|\psi_{0,\mathrm{Max}}^{(N)}\rangle = 0$, and the superscript "O" indicates that we have completed the first step of optimization. At this point, the full-space quantum state after subspace optimization is $|\psi_0^{\mathrm{O}}\rangle = \bigoplus_{N=0}^{\infty} C_N |\psi_{0,\mathrm{Max}}^{(N)}\rangle$. At present, the quantum state of each subspace is given by Eq. (14). Next, we investigate the optimization of the probability distribution for each subspace.

3.2.2. Optimization of subspace probability distribution

Interestingly, we note that $\mathcal{F}_g$ is positively correlated with the excitation number N. As a result, as long as the photon number of the optical field is continuously increased, the QFI becomes larger, resulting in higher estimation precision. However, the intensity of the optical field that can be achieved in the experiment is limited. This means that the optimization of the excitation number distribution P_N should be based on the premise that the average excitation number remains unchanged. Currently, we limit the average number of excitations to $\bar{N}$ and discuss them separately in the case of large and small detunings where $\bar{N} = \sum_{N=0}^{\infty} P_N N$.

In the case of small detuning, by Eq. (15) the maximum QFI in the subspace is approximately

$$F_{g,\mathrm{Max}}^{(N)} = \frac{16N^2 g^2 t^2}{\Delta^2 + 4Ng^2} \approx 4Nt^2. \tag{21}$$

One can find that $F_{g,\mathrm{Max}}^{(N)}$ is approximately proportional to the excitation number N. As a result, when the average excitation number is restricted to $\bar{N}$, the QFI of the subspace corresponding to the excitation number distributions P_N reads as $\mathcal{F}_g^{\mathrm{O}} \approx 4\bar{N}t^2$.

In the situation of large detuning, the maximum QFI in the subspace is approximately

$$F_{g,\mathrm{Max}}^{(N)} \approx \frac{16N^2g^2t^2}{\Delta^2}. \tag{22}$$

Namely, $F_{g,\mathrm{Max}}^{(N)}$ is approximately proportional to the square of the excitation number. Therefore, when the average excitation number $\bar{N}$ is determined, the larger the variance of the excitation number, the greater the $\mathcal{F}_g^{\mathrm{O}}$.

To study the limiting QFI under increasing excitation number fluctuation $\Delta\hat{N}$, we define a binary state,

$$|\psi_0^{\mathrm{O,bs}}\rangle = \sqrt{P_0}|g,0\rangle + \sqrt{P_N}\frac{|e,N-1\rangle + i|g,N\rangle}{\sqrt{2}}. \tag{23}$$

The superscript "bs" indicates that the probabilities are distributed only in the subspace corresponding to the minimum $N=0$ and the maximum N excitation numbers with probabilities P_0 and $P_N = 1 - P_0$, respectively. Note that in order to meet the requirement that the average excitation number is $\bar{N}$, $P_N = \bar{N}/N$ is required. In the current situation, the QFI of g in the whole space is

$$\mathcal{F}_g^{\mathrm{O,bs}} = P_0F_{g,\mathrm{Max}}^{(0)} + P_NF_{g,\mathrm{Max}}^{(N)} = \frac{\bar{N}}{N}\frac{16N^2g^2t^2}{\Delta^2 + 4g^2N}. \tag{24}$$

In Fig. 2, we plot the variation of whole space $\mathcal{F}_g^{\mathrm{O,bs}}$ and the excitation number variance ΔN^2 over N. We can clearly see that in the case of $4Ng^2 \ll \Delta^2$ (large detuning), $\mathcal{F}_g^{\mathrm{O,bs}}$ is proportional to the variance of the excitation number. However, as N continues to increase, the approximate $4Ng^2 \ll \Delta^2$ gradually fails, and at this point $\mathcal{F}_g^{\mathrm{O,bs}}$ gradually approaches the limit value $\lim_{N\to\infty}\mathcal{F}_g^{\mathrm{O,bs}} = 4\bar{N}t^2$, which is the same as the result in the case of small detuning.

3.2.3. Performance of direct-product state

According to the previous section, the optical field in the optimized quantum state $|\psi_g^{\mathrm{O}}\rangle$ is highly entangled with the atom, which leads to difficulties in preparation. Considering the experimental ease of preparation of the direct-product state, in this section, we look for a direct-product state $|\psi_g^{\mathrm{P}}\rangle$ to substitute. Suppose the form of the direct-product state is

$$|\psi_0^{\mathrm{P}}\rangle = |\psi_o\rangle \otimes |\psi_a\rangle, \tag{25}$$

with

$$|\psi_o\rangle = \sum_{n=0}^{\infty}|c_n|e^{i\phi n}|n\rangle, \quad |\psi_a\rangle = \frac{1}{\sqrt{2}}(|e\rangle + e^{-i\chi}|g\rangle), \tag{26}$$

where $|\psi_o\rangle$ and $|\psi_a\rangle$ are quantum states of the optical field and the atom, respectively; χ is the relative phase between the ground and excited states of the atom; and ϕ is the phase difference between the adjacent optical Fock states. In particular, we let the phase of the complex amplitude c_n be linear with the photon number and follow a Gaussian distribution ($\bar{n}$ and Δn^2 are the mean and variance, respectively), satisfying $|c_n|^2 = N\exp[-(n-\bar{n})^2/(2\Delta n^2)]$. This is because some typical quantum states in quantum optics meet this assumption, such as large amplitude coherent states and squeezed states with large squeezing degrees.

In comparing the effects of replacing $|\psi_0^{\mathrm{P}}\rangle$ with $|\psi_0^{\mathrm{O}}\rangle$, we find that a reasonable limitation is that the average excitation number and excitation number fluctuations satisfy $\bar{N} = \bar{n} + 1/2$ and $\Delta N = \Delta n$, respectively. For this reason, we also assume that the excitation number distribution of the optimized state satisfies the Gaussian type[34,35,51], i.e., $P_N = \mathcal{N}\exp[-(N-\bar{N})^2/(2\Delta N^2)]$. We label the QFI corresponding to states $|\psi_0^{\mathrm{P}}\rangle$ and $|\psi_0^{\mathrm{O}}\rangle$ as $\mathcal{F}_g^{\mathrm{P}}$ and $\mathcal{F}_g^{\mathrm{O}}$, respectively.

As shown in Fig. 3, we have drawn the phase diagram of $\mathcal{R} = \mathcal{F}_g^{\mathrm{P}}/\mathcal{F}_g^{\mathrm{O}}$ as a function of the phase difference and particle number fluctuation. Obviously, the larger $\mathcal{R}$ means that the direct-product state $|\psi_0^{\mathrm{P}}\rangle$ is closer to the optimal state $|\psi_0^{\mathrm{O}}\rangle$ in effect. From Fig. 3, one can find that when the phase difference between

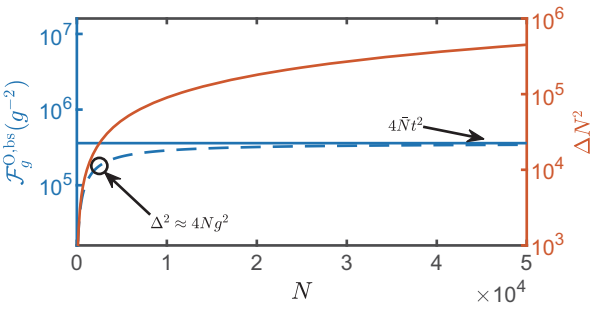

Fig. 2. Blue dashed line depicts the variation of $\mathcal{F}_g^{\mathrm{O,bs}}$ with respect to the excitation number N. The blue solid line is for the limit case of small detuning, while the orange solid line represents the variation of variance ΔN^2 with respect to N. Here, we set $\bar{N} = 10$, $gt = 100$, and $\Delta = 100g$.

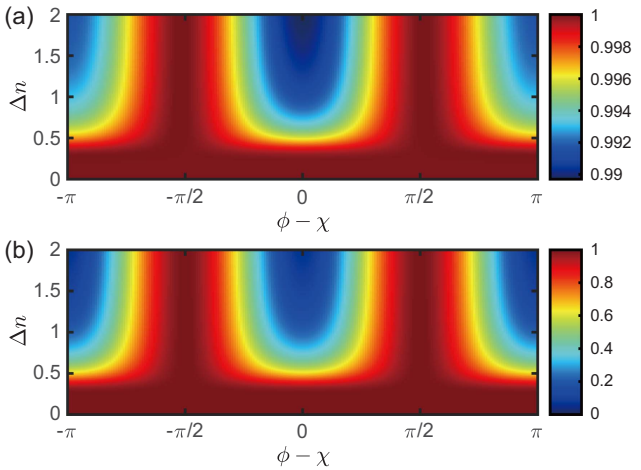

Fig. 3. Density plot of $\mathcal{R} = \mathcal{F}_g^{\mathrm{P}}/\mathcal{F}_g^{\mathrm{O}}$ versus the phase difference and particle number fluctuation. (a) Large detuning with $\Delta = 200g$. (b) Small detuning with $\Delta = 0$ (resonance between the atom and the optical field). Other parameters are $gt = 100$ and $\bar{n} = 100$.

the optical field and the atom is fixed at $\phi - \chi = \pm\pi/2, \mathcal{R} \approx 1$. In the case of large detuning, this phase-matching condition is much more relaxed, and $\mathcal{R}$ does not drop much in the mismatch region. This indicates that the direct-product state we construct is approximately the optimal state in the current situation.

Finally, we investigate the impact of different initial states of the optical field on estimation precision. Here, we mainly consider coherent states, amplitude-squeezed states, and phase-squeezed states.

Case I: Assume that the initial state of the optical field is a coherent state, i.e., $|\psi_o\rangle \propto \sum \frac{\alpha^n}{\sqrt{n}}|n\rangle$[34,35]. At present, the phase difference between the adjacent Fock states is the phase of the coherent state. Therefore, for the coherent state optical field, only the phase difference between its complex amplitude and the atomic phase is $\pm\pi/2$ to achieve the effect of subspace optimization.

Case II: Suppose the initial state of the optical field is a squeezed coherent state, i.e., $|\psi_o\rangle = D(\alpha)S(\xi)|0\rangle$. Here, $D(\alpha) = \exp(\alpha a^\dagger - \alpha^* a)$ denotes the displacement operator[34,35], and $S(\xi) = \exp[(\xi^* a^2 - \xi a^{\dagger 2})/2]$ is the squeezed operator[34,35], in which the squeezed parameter is defined as $\xi = r\exp(i\theta)$. In the case that the displacement parameter α is real, $\theta = 0$ and $\theta = \pi$ correspond to an amplitude-squeezed state and a phase-squeezed state, respectively. Note that the phase difference between the complex amplitudes of the adjacent Fock states in the squeezed states is usually not exactly constant and is difficult to calculate. But in the case of strong squeezing, the phase difference is approximately $\phi = \theta/2$. In the case of small squeezing, the phase difference of the neighboring Fock states is approximately constant in the region where the photon number is mainly distributed. Therefore, we numerically calculate the phase difference between the adjacent Fock states in the main distribution region of the particle numbers and then adjust the atomic phase based on this phase difference to meet $\phi - \chi = \pm\pi/2$.

Figure 4 plots the QFI as a function of encoding time t for the different quantum states of the optical fields, including the coherent state, the amplitude-squeezed state, and the phase-squeezed state. In Fig. 4(a), we can see that the three lines overlap. This indicates that when the atom resonates with the optical field and the average number of photons remains the same, the estimation precision obtained by using the three different quantum optical states as initial states to estimate the coupling strength g is the same. The physical mechanism behind this is that when the detuning is very small, the maximum QFI of each subspace is proportional to the excitation numbers. Therefore, when the average excitation number is equal, the QFI of the whole space is completely equal. In addition, it can satisfy the subspace optimal state, owing to the quantum state we choose, and meet the phase matching requirements, which lead to the coinciding of three curves in the figure. However, in the large detuning case, as shown in Fig. 4(b), even though the average number of photons of the three quantum optical field states is the same, there is a bias in the estimation precision given by using them as initial states. We find that under the same

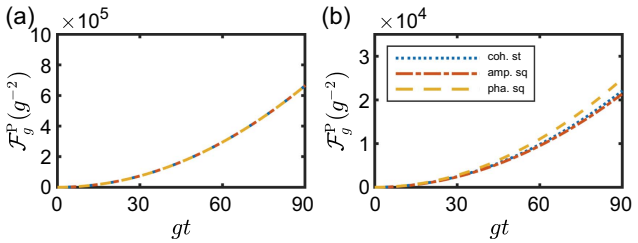

Fig. 4. $\mathcal{F}_g^{\mathrm{P}}$ as a function of encoding time t for the different quantum states of optical fields, which (a) in the case of small detuning is $\Delta = 0$ and (b) in the case of large detuning is $\Delta = 50g$. The complex amplitude of the coherent state is $\alpha = \sqrt{20}e^{i\pi/2}$, and the corresponding atomic state is $(|e\rangle + |g\rangle)/\sqrt{2}$. The squeezed amplitude of the squeezed states is $r = 0.7$. When the squeezed angles are $\theta = 0$ (amplitude-squeezed state) and $\theta = \pi$ (phase-squeezed state), the corresponding atomic states are $(|e\rangle + e^{-i\pi/2}|g\rangle)/\sqrt{2}$ and $(|e\rangle + e^{i\pi/2}|g\rangle)/\sqrt{2}$, respectively. Importantly, for the sake of fairness, it is necessary to set the average number of photons to be the same for different optical field states, i.e., $\alpha = \sqrt{20 - \sinh(r)^2}$.

resources, the phase-squeezed state has the best effect in estimating coupling strength, while the amplitude-squeezed state has the worst effect. Physically, as mentioned earlier, in the case of large detuning, the maximum QFI of the subspace is proportional to the square of the excitation number. Therefore, when the average excitation number is the same, the larger the fluctuation ΔN of the excitation number, the larger QFI of the whole space. Notice that under the same average excitation number, the photon number fluctuation in the amplitude-squeezed state is the smallest, while the photon number fluctuation in the phase-squeezed state is the largest. The phase-squeezed state is thus superior to the other two states when estimating the coupling strength.

Comparing Figs. 4(a) and 4(b), we can find that the precision of estimating the coupling strength g is higher under the resonance condition. In particular, the estimation precision given by the three quantum optical states is the same under the resonance condition. Therefore, in the experiment, one can obtain a high-precision estimation of coupling strength through an easily prepared coherent-stated optical field, which has great practical significance.

4. Conclusion

In summary, we have investigated the parameter estimation and initial state optimization problems in the J–C model. We found that, unlike most parameter estimation studies where the optimal initial state depends on the specific parameter values, there exists a parameter-independent optimal initial state after long-time evolution. This result has practical implications for the application of optimized initial states. Given the large state space of the J–C model, we separated the optimization problem into two steps based on the block-diagonal property of the Hamiltonian equation. Specifically, we optimized the quantum

state of each subspace in the first step and optimized the excitation number distribution of the entire space in the second step. Finally, we found a direct-product state that can replace the highly-entangled optimal initial state to achieve the highest estimation precision, and we investigated the estimation results of several common photon-number statistics distributions under large and small detuning. Our findings showed that, under the resonant condition between the field and the atom, coherent states can be used as initial states to achieve the ultimate estimation precision by controlling the phase difference between the light field and the atom. As for the experimental measurement scheme, the highest possible estimation precision can be achieved by performing positive operator valued measure (POVM) on the final state ρ_g with the eigenvectors of the symmetric logarithmic derivative operator whose expression is $\hat{L}_g = 2\partial_g\rho_g$ in the pure-state case.

Acknowledgement

This work was supported by the Innovation Program for Quantum Science and Technology (No. 2021ZD0303200); the National Key Research and Development Program of China (No. 2016YFA0302001); the National Natural Science Foundation of China (Nos. 11974116, 12234014, and 11654005); the Shanghai Municipal Science and Technology Major Project (No. 2019SHZDZX01); the Fundamental Research Funds for the Central Universities; the Chinese National Youth Talent Support Program; and the Shanghai Talent Program.

References

1. C. L. Degen, F. Reinhard, and P. Cappellaro, "Quantum sensing," Rev. Mod. Phys. **89**, 035002 (2017).
2. V. Giovannetti, S. Lloyd, and L. Maccone, "Advances in quantum metrology," Nat. Photonics **5**, 222 (2011).
3. J. Liu, H. Yuan, X.-M. Lu, and X. Wang, "Quantum fisher information matrix and multiparameter estimation," J. Phys. A **53**, 023001 (2020).
4. R. A. Fisher, *Theory of Statistical Estimation*, Vol. **22** (Cambridge University Press, 1925), p. 700.
5. C. W. Helstrom, "Quantum detection and estimation theory," J. Stat. Phys. **1**, 231 (1969).
6. A. S. Holevo, *Probabilistic and Statistical Aspects of Quantum Theory* (Edizioni della Normale, 2011).
7. M. G. A. Paris, "Quantum estimation for quantum technology," Int. J. Quantum Inf. **7**, 125 (2009).
8. R. Demkowicz-Dobrzański, M. Jarzyna, and J. Kołodyński, "Quantum limits in optical interferometry," Prog. Opt. **60**, 345 (2015).
9. X.-X. Jing, J. Liu, W. Zhong, and X.-G. Wang, "Quantum fisher information of entangled coherent states in a lossy Mach–Zehnder interferometer," Commun. Theor. Phys. **61**, 115 (2014).
10. S. Pang and T. A. Brun, "Quantum metrology for a general Hamiltonian parameter," Phys. Rev. A **90**, 022117 (2014).
11. X. Yu, X. Zhao, L. Shen, Y. Shao, J. Liu, and X. Wang, "Maximal quantum fisher information for phase estimation without initial parity," Opt. Express **26**, 16292 (2018).
12. M. G. Genoni, S. Olivares, and M. G. A. Paris, "Optical phase estimation in the presence of phase diffusion," Phys. Rev. Lett. **106**, 153603 (2011).
13. U. Dorner, R. Demkowicz-Dobrzanski, B. J. Smith, J. S. Lundeen, W. Wasilewski, K. Banaszek, and I. A. Walmsley, "Optimal quantum phase estimation," Phys. Rev. Lett. **102**, 040403 (2009).
14. Z. Hou, Y. Jin, H. Chen, J.-F. Tang, C.-J. Huang, H. Yuan, G.-Y. Xiang, C.-F. Li, and G.-C. Guo, ""Super-Heisenberg" and Heisenberg scalings achieved simultaneously in the estimation of a rotating field," Phys. Rev. Lett. **126**, 070503 (2021).
15. Z. Hou, J.-F. Tang, H. Chen, H. Yuan, G.-Y. Xiang, C.-F. Li, and G.-C. Guo, "Zero–trade-off multiparameter quantum estimation via simultaneously saturating multiple Heisenberg uncertainty relations," Sci. Adv. **7**, eabd2986 (2021).
16. C. Sanavio, J. Z. Bernád, and A. Xuereb, "Fisher-information-based estimation of optomechanical coupling strengths," Phys. Rev. A **102**, 013508 (2020).
17. Z. Sun, J. Ma, X.-M. Lu, and X. Wang, "Fisher information in a quantum-critical environment," Phys. Rev. A **82**, 022306 (2010).
18. K. Sala, T. Doicin, A. D. Armour, and T. Tufarelli, "Quantum estimation of coupling strengths in driven-dissipative optomechanics," Phys. Rev. A **104**, 033508 (2021).
19. J. Yang, S. Pang, Y. Zhou, and A. N. Jordan, "Optimal measurements for quantum multiparameter estimation with general states," Phys. Rev. A **100**, 032104 (2019).
20. A. Carollo, B. Spagnolo, A. A. Dubkov, and D. Valenti, "On quantumness in multi-parameter quantum estimation," J. Stat. Mech. **2019**, 094010 (2019).
21. M. Szczykulska, T. Baumgratz, and A. Datta, "Multi-parameter quantum metrology," Adv. Phys. X **1**, 621 (2016).
22. R. Demkowicz-Dobrzański, W. Górecki, and M. Guță, "Multi-parameter estimation beyond quantum Fisher information," J. Phys. A **53**, 363001 (2020).
23. T. J. Proctor, P. A. Knott, and J. A. Dunningham, "Multiparameter estimation in networked quantum sensors," Phys. Rev. Lett. **120**, 080501 (2018).
24. J. J. Meyer, J. Borregaard, and J. Eisert, "A variational toolbox for quantum multi-parameter estimation," npj Quantum Inf. **7**, 89 (2021).
25. M. Tsang, R. Nair, and X.-M. Lu, "Quantum theory of superresolution for two incoherent optical point sources," Phys. Rev. X **6**, 031033 (2016).
26. K. Liang, S. Wadood, and A. N. Vamivakas, "Quantum Fisher information for estimating N partially coherent point sources," Opt. Express **31**, 2726 (2023).
27. J. Shao and X.-M. Lu, "Performance-tradeoff relation for locating two incoherent optical point sources," Phys. Rev. A **105**, 062416 (2022).
28. Y. Zhou, J. Yang, J. D. Hassett, S. M. H. Rafsanjani, M. Mirhosseini, A. N. Vamivakas, A. N. Jordan, Z. Shi, and R. W. Boyd, "Quantum-limited estimation of the axial separation of two incoherent point sources," Optica **6**, 534 (2019).
29. P. C. Humphreys, M. Barbieri, A. Datta, and I. A. Walmsley, "Quantum enhanced multiple phase estimation," Phys. Rev. Lett. **111**, 070403 (2013).
30. J.-D. Yue, Y.-R. Zhang, and H. Fan, "Quantum-enhanced metrology for multiple phase estimation with noise," Sci. Rep. **4**, 5933 (2014).
31. C. N. Gagatsos, D. Branford, and A. Datta, "Gaussian systems for quantum-enhanced multiple phase estimation," Phys. Rev. A **94**, 042342 (2016).
32. A. Z. Goldberg, I. Gianani, M. Barbieri, F. Sciarrino, A. M. Steinberg, and N. Spagnolo, "Multiphase estimation without a reference mode," Phys. Rev. A **102**, 022230 (2020).
33. Y. Yao, L. Ge, X. Xiao, X.-G. Wang, and C.-P. Sun, "Multiple phase estimation in quantum cloning machines," Phys. Rev. A **90**, 022327 (2014).
34. W. Vogel and D.-G. Welsch, *Quantum Optics* (Wiley-VCH, 2006).
35. P. Meystre and M. Sargent III, *Elements of Quantum Optics*, 4th ed. (Springer-Verlag, 2007).
36. M. Yönaç, T. Yu, and J. H. Eberly, "Sudden death of entanglement of two Jaynes–Cummings atoms," J. Phys. B At. Mol. Opt. Phys. **39**, S621 (2006).
37. A. K. Rajagopal, K. L. Jensen, and F. W. Cummings, "Quantum entangled supercorrelated states in the Jaynes–Cummings model," Phys. Lett. A **259**, 285 (1999).
38. S. J. Akhtarshenas and M. Farsi, "Negativity as entanglement degree of the Jaynes–Cummings model," Phys. Scr. **75**, 608 (2007).
39. J. Gea-Banacloche, "Collapse and revival of the state vector in the Jaynes–Cummings model: an example of state preparation by a quantum apparatus," Phys. Rev. Lett. **65**, 3385 (1990).

40. N. Metwally, M. Abdelaty, and A.-S. Obada, "Quantum teleportation via entangled states generated by the Jaynes–Cummings model," Chaos Solitons Fractals **22**, 529 (2004).
41. J.-M. Liu and B. Weng, "Approximate teleportation of an unknown atomic state in the two-photon Jaynes–Cummings model," Physica A **367**, 215 (2006).
42. F. Mirmasoudi and S. Ahadpour, "Dynamics super quantum discord and quantum discord teleportation in the Jaynes–Cummings model," J. Mod. Opt. **65**, 730 (2018).
43. M. G. Genoni and C. Invernizzi, "Optimal quantum estimation of the coupling constant of Jaynes–Cummings interaction," Eur. Phys. J. Spec. Top. **203**, 49 (2012).
44. K. E. Anouz, A. E. Allati, A. Salah, and F. Saif, "Quantum Fisher information: probe to measure fractional evolution," Int. J. Theor. Phys. **59**, 1460 (2020).
45. A. Houssaoui, K. E. Anouz, and A. E. Allati, "Study of quantum Fisher information matrix and multiparameter estimation for an atomic-field system," Eur. Phys. J. Plus **138**, 109 (2023).
46. V. Giovannetti, S. Lloyd, and L. Maccone, "Quantum metrology," Phys. Rev. Lett. **96**, 010401 (2006).
47. D. C. Brody and E.-M. Graefe, "Information geometry of complex Hamiltonians and exceptional points," Entropy **15**, 3361 (2013).
48. S. L. Braunstein, C. M. Caves, and G. J. Milburn, "Generalized uncertainty relations: theory, examples, and Lorentz invariance," Ann. Phys. **247**, 135 (1996).
49. E. Merzbacher, *Quantum Mechanics*, 3rd ed. (Wiley & Sons, 1998).
50. F. Schwabl, *Quantum Mechanics*, 4th ed. (Springer-Verlag, 2007).
51. T. Radożycki, "A concise and universal method for deriving arbitrary paraxial and d'Alembertian cylindrical Gaussian-type light modes," Opt. Laser Technol. **147**, 107670 (2022).